Research Square

Preprints are preliminary reports that have not undergone peer review.
They should not be considered conclusive, used to inform clinical practice,
or referenced by the media as validated information.

Disruption of Oxaloacetate Acetylhydrolase Impairs Lignocellulose Utilization but Enhances Mycelial Material Properties in Perenniporia fraxinea

Yeon-Jae Choi
Gyeongsang National University
Hyerang Eom
Gyeongsang National University
Seong Hyeok Yang
Gyeongsang National University
Dong Hee Kim
Gyeongsang National University
Beomgyu Park
Gyeongsang National University
Hyun-Jae Shin
Chosun University
Hyeon-Su Ro
rohyeon@gnu.ac.kr

Gyeongsang National University https://orcid.org/0000-0003-1128-8401

Research Article

Keywords: Perenniporia fraxinea, gene editing, oxalic acid, mycelial mat

Posted Date: September 9th, 2026

DOI: https://doi.org/10.21203/rs.3.rs-10825672/v1

License: This work is licensed under a Creative Commons Attribution 4.0 International License.
Read Full License

Abstract

Oxalic acid (OA) plays important roles in fungal nutrient acquisition, environmental acidification, and lignocellulose degradation, but excessive OA accumulation can weaken fungal mycelial materials. In this study, we investigated the physiological and metabolic functions of oxaloacetate acetylhydrolase (OAH), a major OA-producing enzyme, in the white-rot fungus *Perenniporia fraxinea* by disrupting *OAH* using Cas9-sgRNA ribonucleoprotein complexes and donor DNA. *OAH* disruption reduced OA production from 10.5 to 5.1 mM and increased culture pH from 4.8 to 5.4. The *OAH*-disrupted mutant Tf2 showed impaired growth in the presence of insoluble calcium phosphate and markedly reduced growth on oak sawdust and lignin-containing minimal medium. Combined laccase and peroxidase activity decreased to 71% of the WT level but was restored to 93% after adjustment of the culture broth to pH 3.0, indicating that OA-mediated acidification contributes to extracellular oxidative enzyme activity. *OAH* disruption induced extensive transcriptional remodeling of central carbon metabolism, including marked upregulation of TCA- and glyoxylate-pathway genes. Notably, *glyoxylate oxidase* expression increased 16.7-fold, suggesting a compensatory pathway responsible for residual OA production. In contrast to the impaired substrate-utilization phenotypes, Δ*oah*/Δ*oah* mycelial mats exhibited substantially improved mechanical properties, including a 2.9-fold increase in maximum breaking force and increased tensile strength and Young's modulus. These findings demonstrate that OAH-mediated OA production facilitates mineral acquisition and lignocellulose utilization in *P. fraxinea*, while its reduction enhances the mechanical properties of mycelial mats, identifying OA metabolism as a potential target for engineering fungi for mycelium-based biomaterials.

Introduction

Wood-decay fungi, including mushroom-forming fungi, are major decomposers of lignocellulosic biomass and play a central role in carbon cycling in terrestrial ecosystems. In particular, white-rot fungi are among the few organisms capable of efficiently degrading lignin, a major structural component of plant cell walls, and thus play a critical role in the decomposition and recycling of woody biomass in forest ecosystems (Del Cerro et al. 2021; Suryadi et al. 2022). Beyond their ecological importance, fungi have recently attracted increasing attention for their potential applications in sustainable biomaterials, alternative foods, bioremediation, and other emerging fields of biotechnology (Kojima et al. 2026; Shin et al. 2025).

These fungi produce a wide variety of metabolites in responses to different abiotic and biotic stresses. Organic acids are among the major low-molecular-weight compounds produced through both primary and secondary metabolism. They facilitate the solubilization of insoluble inorganic salts and minerals in soil and woody substrates, thereby increasing nutrient availability to fungi, other microorganisms, and plants (Gadd 1999; Gadd et al. 2014; Grąz 2024). Organic acids may also suppress competing microorganisms by lowering the local environmental pH and create acidic conditions favorable for the activity of lignin-degrading enzymes, including laccase, manganese peroxidase, and lignin peroxidase (Grąz et al. 2023; Mäkelä et al. 2002).

Among the various organic acids produced by fungi, oxalic acid (OA) is particularly abundant and plays diverse physiological and ecological roles (Munir et al. 2001). OA is the simplest dicarboxylic acid (pK_{a1} = 1.25, pK_{a2} = 4.28) and is one of the strongest organic acids produced by living organisms. It contributes to the detoxification of excess environmental metal ions through chelation and precipitation as oxalate salts and facilitates the weakening of plant cell walls by chelating cell wall-associated calcium (Dutton et al. 1993). OA can also influence microbial interactions; for example, it has been reported to suppress the growth of competing phytopathogenic bacteria during mushroom cultivation (Kwak et al. 2016). Conversely, OA functions as an important virulence factor in several plant-pathogenic fungi, and its degradation or removal has therefore been explored as a strategy for controlling OA-dependent fungal diseases (Estoppey et al. 2025).

OA production is closely linked to the tricarboxylic acid (TCA) cycle and the glyoxylate cycle and thus influences fungal carbon and energy metabolism (Munir et al. 2001). Oxaloacetate acetylhydrolase (OAH; EC3.7.1.1), which catalyzes the hydrolysis of oxaloacetate to OA and acetate, is a major enzyme involved in fungal OA biosynthesis (Mäkelä et al. 2002; Munir et al. 2001). Expression of the *OAH* gene is developmentally regulated and occurs predominantly in young, actively growing mycelia, whereas it is strongly repressed in older mycelia (Wang et al. 2016). In *Sclerotinia sclerotiorum*, reduced *OAH* expression and OA production in older mycelia are associated with decreased pathogenicity, indicating the importance of *OAH*-mediated OA production in fungal growth and host interactions (Wang et al. 2016).

In industrial applications of fungal mycelia, excessive accumulation of OA can adversely affect the productivity and quality of mycelium-based materials. In particular, OA accumulation has been associated with accelerated weakening of mycelial mats produced by *Ganoderma lucidum* and *Perenniporia fraxinea* (Bae et al. 2021). Therefore, reducing OA production may be advantageous under controlled cultivation conditions for the production of mycelium-based biomaterials. In the present study, we investigated the functions of *OAH* in *P. fraxinea*, a white-rot polypore and plant-pathogenic wood-decay fungus that forms tough, woody, perennial brackets around the bases and roots of hardwood trees. The *OAH* gene was disrupted using a Cas9–sgRNA ribonucleoprotein (RNP) complex together with donor DNA, based on a gene-editing approach previously established for *G. lucidum* (Choi et al. 2025; Eom et al. 2023; Nandre et al. 2025). We examined the effects of *OAH* disruption on OA production, lignin utilization, calcium phosphate utilization, and the formation and physical properties of mycelial mats. In addition, changes in the expression of genes associated with the TCA cycle and glyoxylate cycle were analyzed to investigate the metabolic responses to impaired OA biosynthesis. These analyses provide insight into the physiological roles of *OAH* in white-rot fungi and its potential as a genetic target for modifying the properties of fungal mycelium for biomaterial applications.

Materials and methods

Strains and culture conditions

The dikaryotic strain of *P. fraxinea* 1141 was isolated from stump of Zelcova tree (*Zelcova serrata*) in the Gyeongsang National University campus in August, 2016. A monokaryotic strain M8 was generated by de-dikaryotization using previously reported method (Ha et al. 2019). The strains were cultured in potato dextrose broth (PDB, Difco, NJ, USA) or on PDA (Difco) at 30℃ for most of the experiments with supplementations if needed. Lignin degradation was investigated using a minimal medium composed of $MgSO_4$ (0.5 g/L), KH_2PO_4 (0.46 g/L), K_2HPO_4 (1 g/L), asparagine (2 g/L), thiamine HCl (12 mg/L), and 2% agar with various concentration of lignin (Sigma-Aldrich, St. Luis, MO, USA).

Sawdust medium for the investigation of mycelial development was prepared by mixing 80 g of oak tree sawdust in 20 mL of water. The medium was filled to glass tube (20 cm × 3 cm) and autoclaved at 121℃ for 30 min.

Disruption of OAH gene by Cas9-sgRNA ribonucleoprotein complex

The *OAH* gene and the GPD promoter sequences in *P. fraxinea* were obtained from the genomic sequence of *P. fraxinea* SS3 in Mycocosm (mycocosm.jgi.doe.gov/Perfra1/Perfra1.home.html). The DNA sequences were amplified using the primer sets described in Supplementary Table S1. Construction of donor DNA for OAH disruption was performed by overlap PCR using PCR-amplified DNA fragments, including 5'-HR covering 498-bp sequence region from the start codon, GPD promoter (1,064 bp), hygromycin resistance gene amplified from pHAtC-AbCas9/gRNA (Choi et al. 2023), and 3'-HR containing 465-bp region of 3'-region of OAH (Supplementary Fig. S1 and Fig. 1).

Cas9-sgRNA RNP complexes were employed to induce a targeted double strand break (DSB) in *OAH*. First, the best sgRNA, sgRNA3 targeting Exon6 of *OAH*, among four sgRNA sequences designed using CRISPOR (http://crispor.tefor.net/) was selected by *in vitro* cleavage assay (Supplementary Fig. S2). The Cas9-sgRNA3 RNP complex, assembled by incubation of 10 μg of Cas9 protein and 5 μg of sgRNA3 on ice for 1 h, was introduced to protoplasts (10^7) of *P. fraxinea* 1141 by PEG-mediated transformation with donor DNA (5 μg), as described previously (Choi et al. 2025; Eom et al. 2023). The transformed protoplast solution was spread on PDA plate containing 0.5 M sucrose and incubated at 28℃ for regeneration. PDA containing hygromycin (0.5 mg/mL) was overlayed on top of the PDA plate after 5 days of incubation. The transformants showing hygromycin resistance were isolated and transferred to PDA plate containing hygromycin (0.1 mg/mL) from the overlayed PDA plate while incubating at 30℃ for 3 weeks.

Identification of OAH gene disruption

The *OAH* gene sequence regions of the transformants were amplified using a primer set (OAH_F and OAH_R in Supplementary Table S1) and the PCR amplicons resolved by agarose gel electrophoresis were cloned into TA vector (TOPcloner; Enzynomics, Daejeon, Korea) for sequencing. The verified sequences are described in Supplementary Data S1.

HPLC analysis of oxalic acid

OA in the culture broth was analyzed by HPLC. For this, the culture broth was mixed with the mobile phase (0.1 M sodium sulfate, pH adjusted to 2.65 with methanesulfonic acid) in 1:4 (v/v) ratio. The mixture was filtered through 0.2 mm-syringe filter (Minisart Syringe Filter, Satorius, Göttingen, Germany). The filtrate was analyzed using HPLC system (Ultimate 3000; ThermoFisher Scientific, Seoul, Korea) equipped with Acclaim Organic Acid Column (4 × 150 mm) (ThermoFisher Scientific). The mobile phase was delivered at a flow rate of 0.5 mL/min. The column temperature was maintained at 30°C and the eluent was detected at 210 nm. The oxalic acid concentration was determined using data from three independent experiments.

Enzyme activity assays

Combined laccase and peroxidase activity in culture broth was measured using 2,2'-azino-bis(3-ethylbenzothiazoline-6-sulfonic acid) (ABTS) as the substrate. The reaction mixture containing 5 mM ABTS and 0.3 mL of filtered culture broth was incubated at 25°C for 10 min, and ABTS oxidation was monitored by measuring the absorbance at 420 nm. The ABTS oxidation rate was calculated using molar extinction coefficient 36,000 $M^{-1}cm^{-1}$ of oxidized ABTS.

Quantitative RT-PCR analysis

The mushroom mycelia were frozen in liquid nitrogen and were ground using mortar and pestle. Total RNA was extracted using a MiniBEST plant RNA extraction kit (Takara, Kyoto, Japan). cDNA was synthesized using the extracted RNA and then was subjected to real-time PCR using CronoSTAR™ 96 Real-Time PCR System(4ch) (Clontech, Kyoto, Japan). The condition was as follows: initial denaturation at 95°C for 30 s and 45 cycles of polymerization at 60°C for10 s and denaturation at 95°C for 5 s. The expression level of gene was calculated by $2^{-\Delta\Delta Ct}$ method using a three replicated data set.

Mycelial mat formation and mechanical property analysis

Mycelia were cultured on 400 mL of soft PDA (potato-dextrose agar containing 0.5% agar) in a square dish (24.3 cm × 24.3 cm) (SPL 11245; SPL Life Science, Pocheon, Korea) for 3 weeks at 30°C with 80% relative humidity. The mycelial mat was detached from the agar surface and immersed in a fixation solution containing 1% formaldehyde and 5% glycerol for 12 h at room temperature. The fixed mat was dried at 60°C for 12 h.

Mechanical properties of the mycelial mat were tested using universal testing machine (UTM; AGS-X, Shimadzu, Japan). The tensile strength and elongation were measured at a tensile speed at 5 mm/min to compare the properties of each strain. All samples were cut into 2.0 × 6.0 cm^2 and tested triplicate.

Pairwise comparisons were performed using independent *t*-tests with a confidence level at 0.95, to evaluate the significance of differences between the wild type strain and other groups.

Scanning electron microscopy (SEM) analysis

The dried mycelial mats were sputter coated (Sputter Coater EM SCD500; Leica, Wetzlar, Germany) with a 10 nm gold/palladium layer. Scanning electron microscopy (SEM) was performed using a Thermo Scientific Apreo 2 S field-emission scanning electron microscope (FE-SEM). Images were acquired using an Everhart–Thornley secondary electron detector (ETD) at an accelerating voltage of 20 kV, a working distance of 8.0 mm, and a beam current of 50 pA. Mat thickness, surface area, and hyphal width were measured from the corresponding digital and SEM images using ImageJ software (National Institutes of Health, Bethesda, MD, USA).

Statistical analysis

All experiments were performed with at least three independent replicates. Statistical significance between the WT and Δ*oah*/Δ*oah* strains was evaluated using independent two-sample *t*-tests at a 95% confidence level. Statistical significance was indicated as $p \leq 0.05$ (*), $p \leq 0.01$ (**), and $\mathbf{p} \leq 0.001$ (***).

Results

Disruption of OAH by Cas9-sgRNA RNP complex with donor DNA

The *OAH* gene in *P. fraxinea* 1141 was disrupted by introducing donor DNA together with Cas9-sgRNA RNP complexes. A total of 12 transformants were obtained, and successful insertion of the donor DNA at the *OAH* locus was confirmed by PCR and sequencing (Fig. 1 and Supplementary Data S1). The transformation efficiency was similar to that reported in a previous gene-editing study using dikaryotic *Ganoderma lucidum* (Choi et al. 2025). Of the 12 transformants, 11 were dikaryotic, containing both a wild-type nucleus and an *OAH*-disrupted nucleus, whereas one transformant was monokaryotic (Tf2 in Fig. 1B and C).

Karyotyping of the transformants, based on sequence variations in the *homoaconitase* gene and single-nucleotide polymorphism (SNP) in the *OAH* gene that distinguish the A1 and A2 nuclei (Supplementary Fig. S3), classified the transformants into three nuclear genotypes: (1) dikaryotic transformants carrying a wild-type A1 nucleus and an *OAH*-disrupted A2 nucleus, (2) dikaryotic transformants carrying an *OAH*-disrupted A1 nucleus and a wild-type A2 nucleus, and (3) a monokaryotic transformant carrying an *OAH*-disrupted A1 nucleus (Tf2) (Fig. 1). The monokaryotic transformant Tf2 was selected for further characterization and compared with a wild-type monokaryotic strain (M8) carrying the same A1 nuclear genotype.

Oxalic acid production and salt solubilization of the OAH-disrupted mutant

Since OAH catalyzes the hydrolysis of oxaloacetate to OA and acetate, OA production by the *OAH*-disrupted mutant Tf2 was examined by HPLC using authentic OA as a standard. Quantification of OA in the culture broth revealed that the WT strain produced 10.5 mM (0.95 g/L) OA, a level comparable to the 0.7 g/L previously reported for *Lentinula edodes* (Kwak et al. 2016) (Fig. 2A). Disruption of *OAH* did not completely abolish OA production, as Tf2 still produced 5.1 mM (0.46 g/L) OA, corresponding to approximately 49% of the WT level. This residual OA production was comparable to that reported for an *OAH*-deletion mutant of *S. sclerotiorum* (0.65 g/L) (Estoppey et al. 2025). Consistent with the reduced OA production, the culture broth of Tf2 exhibited a higher pH (5.4) than that of the WT strain (4.8) (Fig. 2B).

Environmental acidification can facilitate mineral acquisition by promoting the solubilization of poorly soluble mineral salts. To investigate whether disruption of *OAH* affects the ability to utilize insoluble phosphate, mycelial growth was examined on PDA supplemented with various concentrations of calcium phosphate [$Ca_3(PO_4)_2$], a poorly soluble source of both calcium and phosphate. Mycelial growth of the WT strain was not significantly affected by calcium phosphate supplementation, whereas Tf2 exhibited significantly reduced growth under these conditions (Fig. 2C, D). This growth defect appeared to be associated with an impaired ability to utilize insoluble calcium phosphate, because Tf2 grew normally when supplied with soluble calcium or phosphate salts in the form of $CaCl_2$ or Na_3PO_4, respectively. Notably, $CaCl_2$ promoted the growth of Tf2 in a concentration-dependent manner (Fig. 2D), suggesting that calcium availability may influence the growth phenotype associated with *OAH* disruption.

Growth of the OAH-disrupted mutant on sawdust and lignin

Acidification of woody substrates is known to be prerequisite for substrate decomposition because the activities of several lignin-modifying enzymes, including laccases and lignin peroxidase, are favored under acidic conditions. To investigate whether disruption of *OAH* affects fungal growth on woody substrate, a single mycelial plug (5 × 5 mm) grown on PDA was inoculated onto oak sawdust medium prepared by mixing oak sawdust and distilled water at a ratio of 8:2 (w/w). After 2 weeks of incubation at 30℃, the wild-type (WT) strain exhibited extensive and dense mycelial colonization of the sawdust substrate, whereas Tf2 showed markedly reduced growth and sparse mycelial development (Fig. 3A).

The effect of *OAH* disruption on growth in the presence of lignin was further investigated using minimal medium supplemented with different concentrations of lignin as the sole carbon source. The strains were inoculated onto the medium and incubated for 1 week at 30℃. The WT strain exhibited substantial mycelial growth at lignin concentrations of up to 2 g/L, whereas growth gradually decreased at higher concentrations (Fig. 3B). In contrast, Tf2 exhibited little or no detectable mycelial growth at any of the lignin concentrations tested (Fig. 3B). These results indicate that disruption of *OAH* severely impairs mycelial growth on both oak sawdust and lignin-containing minimal medium, suggesting that *OAH*-mediated OA production contributes to efficient colonization and utilization of woody substrates.

Laccases and peroxidases are important secreted enzymes involved in the oxidative degradation of lignin (D'souza et al. 1999; Hariharan and Nambisan 2013; Higuchi 2004). The combined activity of laccases and peroxidases in the culture broth, as determined by ABTS oxidation, was 7.7 μM/min in Tf2, corresponding to 71% of the WT activity (10.9 μM/min) (Fig. 3C, left panel), despite the higher extracellular protein concentration in the Tf2 culture broth (38 μg/mL) than that of the WT (28 μg/mL) (Fig. 3D). When the pH of the culture broths was adjusted to 3.0 with sodium phosphate buffer, the activity of Tf2 increased to 93% of the WT level, indicating that the reduced extracellular oxidative enzyme activity in Tf2 was largely attributable to the higher culture pH resulting from decreased OA production (Fig. 3C, right panel).

The reduced extracellular enzyme activity of Tf2 is consistent with its impaired mycelial development on sawdust (Fig. 3A) and reduced ability to utilize lignin as the sole carbon source (Fig. 3B), supporting an important role for OA in the efficient decomposition and utilization of lignocellulosic substrates by *P. fraxinea*.

Expression of genes involved in oxalic acid synthesis and related metabolic pathways

Expression of genes involved in OA metabolism and related metabolic pathways was investigated by qRT-PCR. All genes examined in the tricarboxylic acid (TCA) cycle were upregulated in Tf2. In particular, *citrate synthase* (1) and *malate dehydrogenase* (8) exhibited 6.44- and 6.74-fold higher expression, respectively, than in the WT (Fig. 4A). In contrast, expression of the *pyruvate carboxylase* gene (13), which is involved in the anaplerotic replenishment of oxaloacetate, was largely unaffected. These results suggest that disruption of *OAH* induces compensatory remodeling of central carbon metabolism, potentially promoting the utilization of oxaloacetate through the TCA cycle rather than its conversion to OA.

Genes involved in the glyoxylate pathway were also markedly upregulated in Tf2. Expression of *isocitrate lyase* (10) and *malate synthase* (11) increased by 3.16- and 3.75-fold, respectively, suggesting enhanced activity of the glyoxylate pathway. The strongest induction was observed for *glyoxylate oxidase* (12), whose expression increased 16.7-fold relative to the WT. Glyoxylate oxidase catalyzes the oxidation of glyoxylate to OA, suggesting that increased glyoxylate metabolism provides an alternative route for OA production in the absence of functional OAH. This marked induction of *glyoxylate oxidase* may therefore explain, at least in part, the residual OA production observed in the *OAH*-disrupted Tf2 strain (Fig. 2A).

Physical properties of mycelial mat produced by the OAH-disrupted mutant

Organic acids can influence the weakening and coloration of mycelial mats, which are important characteristics in the development of mycelium-based biomaterials (Bae et al. 2021; Shin et al. 2025). To investigate the effect of *OAH* disruption on the properties of mycelial mats, a dikaryotic *OAH*-disrupted

mutant (Δ*oah*/Δ*oah*) was generated by di-mon mating of the monokaryotic Tf2 strain with the dikaryotic Tf1 strain using a previously reported method (Kim et al. 2019).

Mycelial mats of the dikaryotic wild-type PF1141 (WT) and the Δ*oah*/Δ*oah* strains were obtained after 3 weeks of incubation at 30°C (Fig. 5A). The fully grown mycelial mat of the Δ*oah*/Δ*oah* strain had a fresh weight of 135.8 g, approximately 1.2-fold higher than that of the WT (118.0 g) (Fig. 5A, B). After drying overnight at 60°C, the weights decreased to 23.6 and 25.8 g for the WT and mutant strains, respectively. Surface area of the mycelial mat decreased to approximately 70% of its original area upon drying (Fig. 5A). The average thickness of the dried mat was 0.61 cm for the WT and 0.86 cm for the Δ*oah*/Δ*oah* strain (Fig. 5C, D).

Interestingly, the mycelial mats of both the WT and mutant strains consisted of two distinct layers differing in mycelial structure (Fig. 5C, D), corresponding to layers of aerial and surface hyphae, respectively (Kuribayashi et al. 2022). The upper layer of the mutant mat (0.46 cm) was approximately twice as thick as that of the WT (0.23 cm), whereas the thicknesses of the bottom layers were similar between the WT (0.38 cm) and mutant (0.40 cm), suggesting that reduced OA production promotes aerial hyphal growth.

Scanning electron microscopy (SEM) revealed the presence of relatively large-diameter (L) and small-diameter (S) hyphae in both layers (Fig. 5C, D). The average widths of L hyphae in the upper and bottom layers were 1.66 and 0.97 μm, respectively, in the WT and 1.71 and 1.03 μm, respectively, in the Δ*oah*/Δ*oah* strain (Supplementary Fig. S4). The widths of S hyphae were approximately 0.25 μm in the WT and 0.21 μm in the mutant strain, regardless of the layer. SEM analysis further revealed that the bottom layer exhibited a denser hyphal network than the upper layer in both strains (Supplementary Fig. S4). Notably, both layers of the Δ*oah*/Δ*oah* mat contained a greater proportion of L hyphae than those of the WT.

The mechanical properties of mycelial mats were evaluated using a universal testing machine (Fig. 5B). The maximum force required to break the mycelial mat increased from 6.0 N in the WT to 17.2 N in the Δ*oah*/Δ*oah* mutant, corresponding to 2.9-fold increase. Similarly, tensile strength increased from 0.4 MPa in the WT to 1.1 MPa in the Δ*oah*/Δ*oah* mutant, while Young's modulus increased from 9.8 to 16.6 MPa. These results indicate that *OAH* disruption results in the formation of mechanically stronger and stiffer mycelial mats, which may be associated with thicker aerial layer with increased L hyphae.

Discussion

OA is an important fungal metabolite involved in environmental acidification, mineral solubilization, lignocellulose degradation, and interactions in ecosystem (Dutton et al. 1993). In this study, we demonstrated that disruption of *OAH*, encoding oxaloacetate acetylhydrolase, in *P. fraxinea* reduced OA accumulation from 10.5 to 5.1 mM (Fig. 2A), confirming that OAH constitutes a major route for OA biosynthesis. The approximately 51% reduction in OA was accompanied by an increase in culture pH from 4.8 to 5.4, demonstrating the contribution of OAH-dependent OA production to extracellular acidification. Importantly, however, OA production was not completely abolished by *OAH* disruption.

Secretion of organic acid provides fungi with an effective mechanism for mobilizing poorly soluble mineral nutrients in their environment (Gadd 1999; Gadd et al. 2014; Grąz 2024). Tf2 exhibited reduced growth when calcium and phosphate were supplied as insoluble $Ca_3(PO_4)_2$ but grew normally when these nutrients were supplied as soluble $CaCl_2$ or Na_3PO_4 (Fig. 2C), suggesting that reduced OA production impaired the ability of Tf2 to mobilize nutrients from insoluble mineral sources. OA also appears to contribute substantially to the ability of *P. fraxinea* to colonize and utilize woody substrates by providing an extracellular environment favorable for lignocellulose-degrading enzymes (Grąz 2024). Combined laccase and peroxidase activity in Tf2 was reduced to 71% of the WT level under the original culture conditions. Importantly, adjustment of the culture broth to pH 3.0 increased the relative activity of Tf2 to 93% of the WT level. This substantial recovery indicates that much of the reduction in oxidative enzyme activity was associated with the altered extracellular pH rather than simply with a loss of enzyme production. These findings are consistent with the impaired colonization of sawdust and utilization of lignin observed in Tf2 (Fig. 3), supporting an important role for OA-mediated acidification in lignocellulose decomposition by *P. fraxinea*.

The transcriptional response to *OAH* disruption indicates that OA metabolism is closely connected to central carbon metabolism. Because OAH diverts oxaloacetate from the TCA cycle through its conversion to OA and acetate (Munir et al. 2001), continuous OA production requires replenishment of oxaloacetate either through TCA cycle or through anaplerotic reactions, such as the direct carboxylation of pyruvate catalyzed by pyruvate carboxylase (Jitrapakdee et al. 2008). Transcriptional analysis of Tf2, showing upregulation of all examined genes in TCA cycle and constant level expression of *pyruvate carboxylase*, suggests that oxaloacetate is replenished by enhanced performance of TCA cycle. Another notable transcriptional response was the upregulation of *isocitrate lyase* (3.16-fold) and *malate synthase* (3.75-fold), two key enzymes of the glyoxylate pathway. The glyoxylate cycle provides an alternative route for replenishing TCA cycle intermediates, with malate synthase catalyzing the condensation of glyoxylate and acetyl-CoA to form malate (Munir et al. 2001). Notably, *glyoxylate oxidase* was strongly upregulated (16.7-fold) in Tf2. Because glyoxylate oxidase catalyzes the oxidation of glyoxylate to OA, its marked induction suggests that a portion of the glyoxylate pool may be redirected toward OA formation in the absence of functional OAH. Activation of this alternative route could therefore account, at least in part, for the residual OA production in Tf2 (Fig. 5), consistent with the residual OA production reported in an *OAH*-deletion mutant of *S. sclerotiorum* (Estoppey et al. 2025).

In contrast to its negative effects on substrate utilization, reduced OA production had a beneficial effect on the mechanical properties of mycelial mats. The *Δoah/Δoah* strain produced mats with a 1.2-fold higher fresh weight than the WT, which may be associated with enhanced TCA-cycle activity and a shift in carbon allocation from OA production toward biomass formation. The *Δoah/Δoah* strain also exhibited significantly enhanced mechanical properties, as demonstrated by increases in maximum breaking force, tensile strength, and Young's modulus. The enhanced mechanical strength of the *Δoah/Δoah* mats may be associated with changes in mat architecture, including increased overall thickness, an approximately twofold increase in the thickness of the upper aerial-hyphal layer, and a higher proportion of large-diameter L hyphae. Moreover, reduced OA accumulation alleviated the coloration of mycelial

mats (Supplementary Fig. S5), consistent with previous reports implicating OA accumulation in the weakening and coloration of fungal mycelial materials (Bae et al. 2021; Shin et al. 2025).

Notably, the *OAH*-disrupted Tf2 mutant exhibited concentration-dependent growth stimulation in the presence of a soluble calcium salt (Fig. 2C). In fungi, Ca^{2+} plays multiple physiological roles, acting as an important second messenger in the regulation of polarized apical growth (Jackson and Heath 1993) and contributing to cell-wall integrity and remodeling (Chardonnet et al. 1999). Because OA readily binds Ca^{2+} and can precipitate it as calcium oxalate, reduced OA production in the *OAH*-disrupted mutant may increase the availability of extracellular Ca^{2+}. Increased Ca^{2+} availability could, in turn, enhance Ca^{2+}-dependent signaling associated with hyphal growth and cell-wall organization. This mechanism may partly account for the increased mycelial biomass and enhanced mechanical strength of the mycelial mats produced by the *OAH*-disrupted strain.

In conclusion, our results reveal a functional trade-off associated with fungal OA production. OAH-mediated OA production benefits *P. fraxinea* physiologically by promoting extracellular acidification, mineral mobilization, lignocellulose-associated enzyme activity, and efficient colonization of woody substrates. Conversely, reducing OA production through *OAH* disruption markedly improves the strength and stiffness of mycelial mats. OAH therefore represents not only a key metabolic determinant of the ecological and degradative functions of *P. fraxinea* but also a potential target for engineering fungal strains for mycelium-based biomaterials. Modulation of OA metabolism may provide a strategy for balancing efficient substrate colonization during biomass production with improved structural properties of the resulting mycelial material.

Declarations

Authorship contribution statement

Yeon Jae Choi: Investigation, Conceptualization, Data curation, Formal analysis, Validation. **Hyerang Eom:** Investigation, Conceptualization, Data curation, Formal analysis, Validation, Draft writing. **Seong Hyeok Yang**: Investigation. **Dong Hee Kim**: Investigation. **Beomgyu Park**: Investigation. **Hyun-Jae Shin**: Investigation, Formal analysis. **Hyeon-Su Ro:** Conceptualization, Data curation, Formal analysis, Writing – original draft, Supervision, Writing – review & editing.

Declaration of Competing Interest

The authors declare that they have no known competing financial interests or personal relationships that could have appeared to influence the work reported in this paper.

Declaration of generative AI and AI-assisted technologies in the writing process

During the preparation of this work the authors used ChatGPT in order to improve language and readability. After using this tool, the authors reviewed and edited the content as needed and takes full responsibility for the content of the publication.

Acknowledgement

This work was supported by a National Research Foundation of Korea (NRF) grant funded by the Korean government (MSIT) (RS-2025-23323638) and New Breeding Technologies Development Program (RS-2024-00322425), Rural Development Administration (RDA), Republic of Korea.

References

1. Bae B, Kim M, Kim S, Ro H-S (2021) Growth characteristics of polyporales mushrooms for the mycelial mat formation. Mycobiology 49(3):280–284. https://doi.org/https://doi.org/10.1080/12298093.2021.1911401
2. Chardonnet C, Sams C, Conway W (1999) Calcium effect on the mycelial cell walls of *Botrytis cinerea*. Phytochemistry 52(6):967–973. https://doi.org/https://doi.org/10.1016/S0031-9422(99)00315-5
3. Choi Y-J, Eom H, Nandre R, Kim M, Oh Y-L, Kim S, Ro H-S (2025) Simultaneous gene editing of both nuclei in a dikaryotic strain of *Ganoderma lucidum* using Cas9-gRNA ribonucleoprotein. J Microbiol 63(1):e:2409006. https://doi.org/10.71150/jm.2409006
4. Choi YJ, Eom H, Yang S-H, Nandre R, Kim S, Kim M, Oh Y-L, Nakazawa T, Honda Y, Ro H-S (2023) Heterokaryosis, the main obstacle in the generation of PPO1-edited *Agaricus bisporus* by CRISPR/Cas9 system. Sci Hortic 318:112095. https://doi.org/10.1016/j.scienta.2023.112095
5. D'souza TM, Merritt CS, Reddy CA (1999) Lignin-modifying enzymes of the white rot basidiomycete *Ganoderma lucidum*. Appl Environ Microbiol 65(12):5307–5313. https://doi.org/https://doi.org/10.1128/aem.65.12.5307-5313.1999
6. Del Cerro C, Erickson E, Dong T, Wong AR, Eder EK, Purvine SO, Mitchell HD, Weitz KK, Markillie LM, Burnet MC (2021) Intracellular pathways for lignin catabolism in white-rot fungi. Proc Natl Acad Sci USA 118(9):e2017381118. https://doi.org/https://doi.org/10.1073/pnas.2017381118
7. Dutton MV, Evans CS, Atkey PT, Wood DA (1993) Oxalate production by Basidiomycetes, including the white-rot species *Coriolus versicolor* and *Phanerochaete chrysosporium*. Applied Microbiol Biotechnol 39(1):5–10. https://doi.org/https://doi.org/10.1007/BF00166839
8. Eom H, Choi Y-J, Nandre R, Han H-G, Kim S, Kim M, Oh Y-L, Nakazawa T, Honda Y, Ro H-S (2023) The Cas9-gRNA ribonucleoprotein complex-mediated editing of pyrG in *Ganoderma lucidum* and unexpected insertion of contaminated DNA fragments. Sci Rep 13(1):11133. https://doi.org/10.1038/s41598-023-38331-2
9. Estoppey A, Vallat-Michel A, Chain PS, Bindschedler S, Junier P (2025) Impact of oxalic acid consumption and pH on the *in vitro* biological control of oxalogenic phytopathogen *Sclerotinia sclerotiorum*. J Fungi 11(3):191. https://doi.org/https://doi.org/10.3390/jof11030191
10. Gadd GM (1999) Fungal production of citric and oxalic acid: importance in metal speciation, physiology and biogeochemical processes. Adv Microb Physiol 41:47–92. https://doi.org/https://doi.org/10.1016/S0065-2911(08)60165-4

11. Gadd GM, Bahri-Esfahani J, Li Q, Rhee YJ, Wei Z, Fomina M, Liang X (2014) Oxalate production by fungi: significance in geomycology, biodeterioration and bioremediation. Fungal Biol Rev 28(2–3):36–55. https://doi.org/10.1016/j.fbr.2014.05.001
12. Grąz M (2024) Role of oxalic acid in fungal and bacterial metabolism and its biotechnological potential. World J Microbiol Biotechnol 40(6):178. https://doi.org/https://doi.org/10.1007/s11274-024-03973-5
13. Grąz M, Ruminowicz-Stefaniuk M, Jarosz-Wilkołazka A (2023) Oxalic acid degradation in wood-rotting fungi. Searching for a new source of oxalate oxidase. World J Microbiol Biotechnol 39(1):13. https://doi.org/https://doi.org/10.1007/s11274-022-03449-4
14. Ha B, Moon YJ, Song Y, Kim S, Kim M, Yoon C-W, Ro H-S (2019) Molecular analysis of *B* mating type diversity in *Lentinula edodes*. Sci Hortic 243:55–63. https://doi.org/https://doi.org/10.1016/j.scienta.2018.08.009
15. Hariharan S, Nambisan P (2013) Optimization of lignin peroxidase, manganese peroxidase, and Lac production from *Ganoderma lucidum* under solid state fermentation of pineapple leaf. BioResources 8(1):250. https://doi.org/https://doi.org/10.15376/BIORES.8.1.250-271
16. Higuchi T (2004) Microbial degradation of lignin: Role of lignin peroxidase, manganese peroxidase, and laccase. Proceedings of the Japan Academy, Series B 80(5):204–214. https://doi.org/https://doi.org/10.2183/pjab.80.204
17. Jackson S, Heath I (1993) Roles of calcium ions in hyphal tip growth. Microbiol Rev 57(2):367–382. https://doi.org/https://doi.org/10.1128/mr.57.2.367-382.1993
18. Jitrapakdee S, St Maurice M, Rayment I, Cleland WW, Wallace JC, Attwood PV (2008) Structure, mechanism and regulation of pyruvate carboxylase. Biochem J 413(3):369–387. https://doi.org/https://doi.org/10.1042/bj20080709
19. Kim S, Song Y, Ha B, Moon YJ, Kim M, Ryu H, Ro H-S (2019) Variable number tandem repeats in the mitochondrial DNA of *Lentinula edodes*. Genes 10(7):542. https://doi.org/10.3390/genes10070542
20. Kojima H, Im H-S, Kawauchi M, Shin H-J, Schiphof K, Tsuji K, Yoshimi A, Tanaka C, Nakazawa T, Honda Y (2026) Molecular breeding alters mycelium material properties in the white-rot fungus *Pleurotus ostreatus*. Applied Microbiol Biotechnol 110(1):64. https://doi.org/https://doi.org/10.1007/s00253-026-13743-y
21. Kuribayashi T, Lankinen P, Hietala S, Mikkonen KS (2022) Dense and continuous networks of aerial hyphae improve flexibility and shape retention of mycelium composite in the wet state. COMPOS PART A-APPL S 152:106688. https://doi.org/10.1016/j.compositesa.2021.106688
22. Kwak AM, Lee IK, Lee SY, Yun BS, Kang HW (2016) Oxalic acid from *Lentinula edodes* culture filtrate: antimicrobial activity on phytopathogenic bacteria and qualitative and quantitative Analyses. Mycobiology 44(4):338–342. https://doi.org/10.5941/MYCO.2016.44.4.338
23. Mäkelä M, Galkin S, Hatakka A, Lundell T (2002) Production of organic acids and oxalate decarboxylase in lignin-degrading white rot fungi. Enzyme Microb Technol 30(4):542–549. https://doi.org/https://doi.org/10.1016/S0141-0229(02)00012-1

24. Munir E, Yoon JJ, Tokimatsu T, Hattori T, Shimada M (2001) A physiological role for oxalic acid biosynthesis in the wood-rotting basidiomycete *Fomitopsis palustris*. Proc Natl Acad Sci USA 98(20):11126–11130. https://doi.org/https://doi.org/10.1073/pnas.191389598
25. Nandre R, Eom H, Choi Y-J, Zhang Y, Ro H-S (2025) CRISPR/Cas9-mediated gene editing in filamentous fungi, focusing on mushrooms and plant-pathogenic fungi. Fungal Biol Rev 54:100446. https://doi.org/https://doi.org/10.1016/j.fbr.2025.100446
26. Shin H-J, Ro H-S, Kawauchi M, Honda Y (2025) Review on mushroom mycelium-based products and their production process: from upstream to downstream. Bioresour Bioprocess 12(1):3. https://doi.org/https://doi.org/10.1186/s40643-024-00836-7
27. Suryadi H, Judono JJ, Putri MR, Eclessia AD, Ulhaq JM, Agustina DN, Sumiati T (2022) Biodelignification of lignocellulose using ligninolytic enzymes from white-rot fungi. Heliyon 8(2). https://doi.org/https://doi.org/10.1016/j.heliyon.2022.e08865
28. Wang J-p, Xu Y-p, Zang X-p, Li S-s, Cai X-z (2016) *Sclerotinia sclerotiorum* virulence is affected by mycelial age via reduction in oxalate biosynthesis. J Integr Agric 15(05):1034. https://doi.org/10.1016/S2095-3119(15)61199-6

Figures

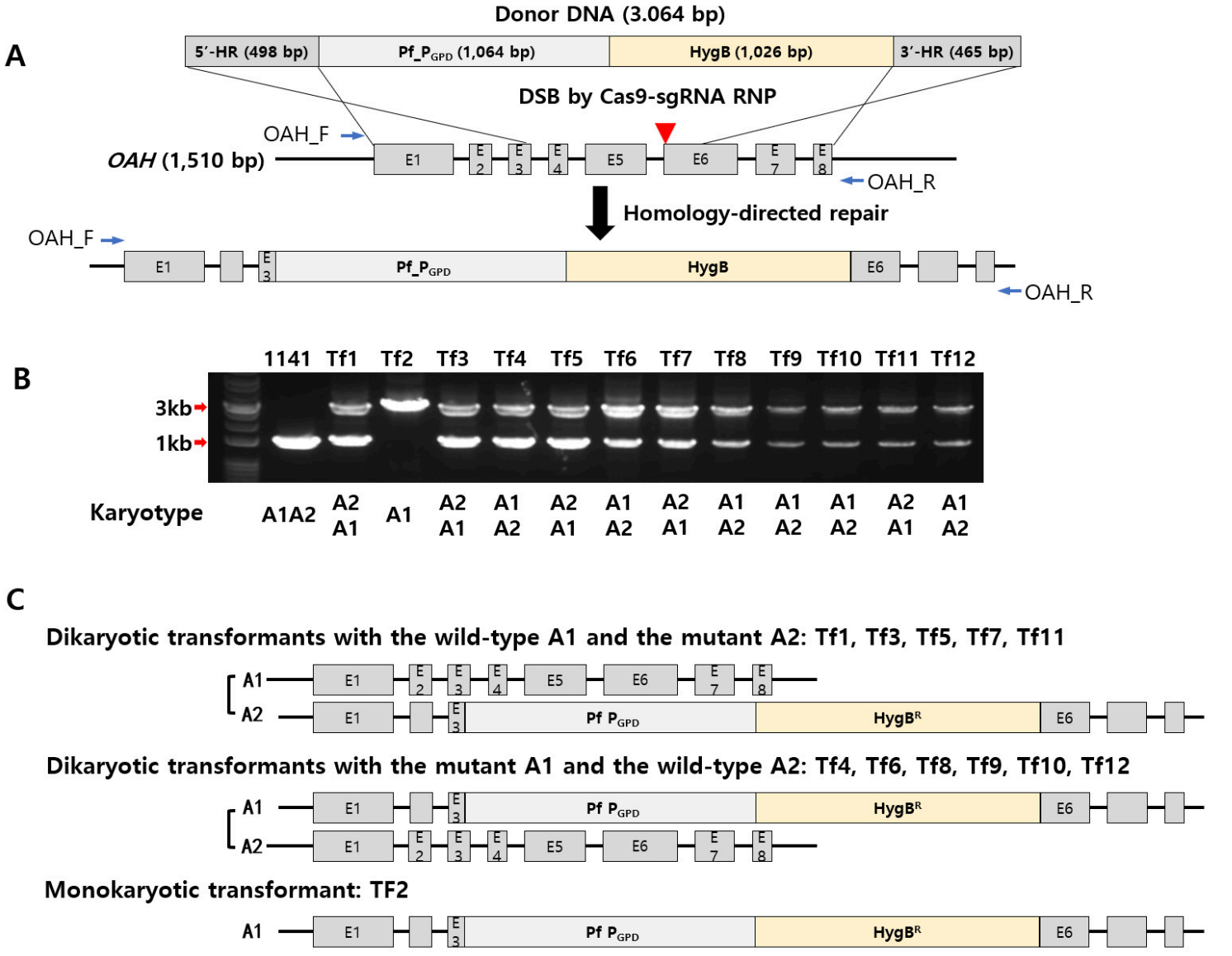


Figure 1

Generation of *OAH*-disrupted mutant strains by Cas9-sgRNA ribonucleoprotein complex with donor DNA. (A) Strategy for *OAH* gene editing. Cas9-sgRNA RNP makes double strand break (DSB) at exon 6 (E6) of *OAH*, as indicated by arrow head. The DSB is repaired using donor DNA by homology-directed repair mechanism. The donor DNA has *P. fraxinea* GPD promoter (Pf_P_{GPD})-hygromycin B resistance gene (*HygB*), flanked by 5′-HR (498 bp) and 3′-HR (465 bp) which are homologous to 5′- and 3′-regions of OAH, respectively. (**B)** PCR amplification of the target *OAH* region in the transformants with primers OAH_F and OAH_R. Karyotypes of the transformants are marked under the gel image. (**C)** Analysis of the transformants. Sequences of the transformants are provided as Supplementary Data S1.

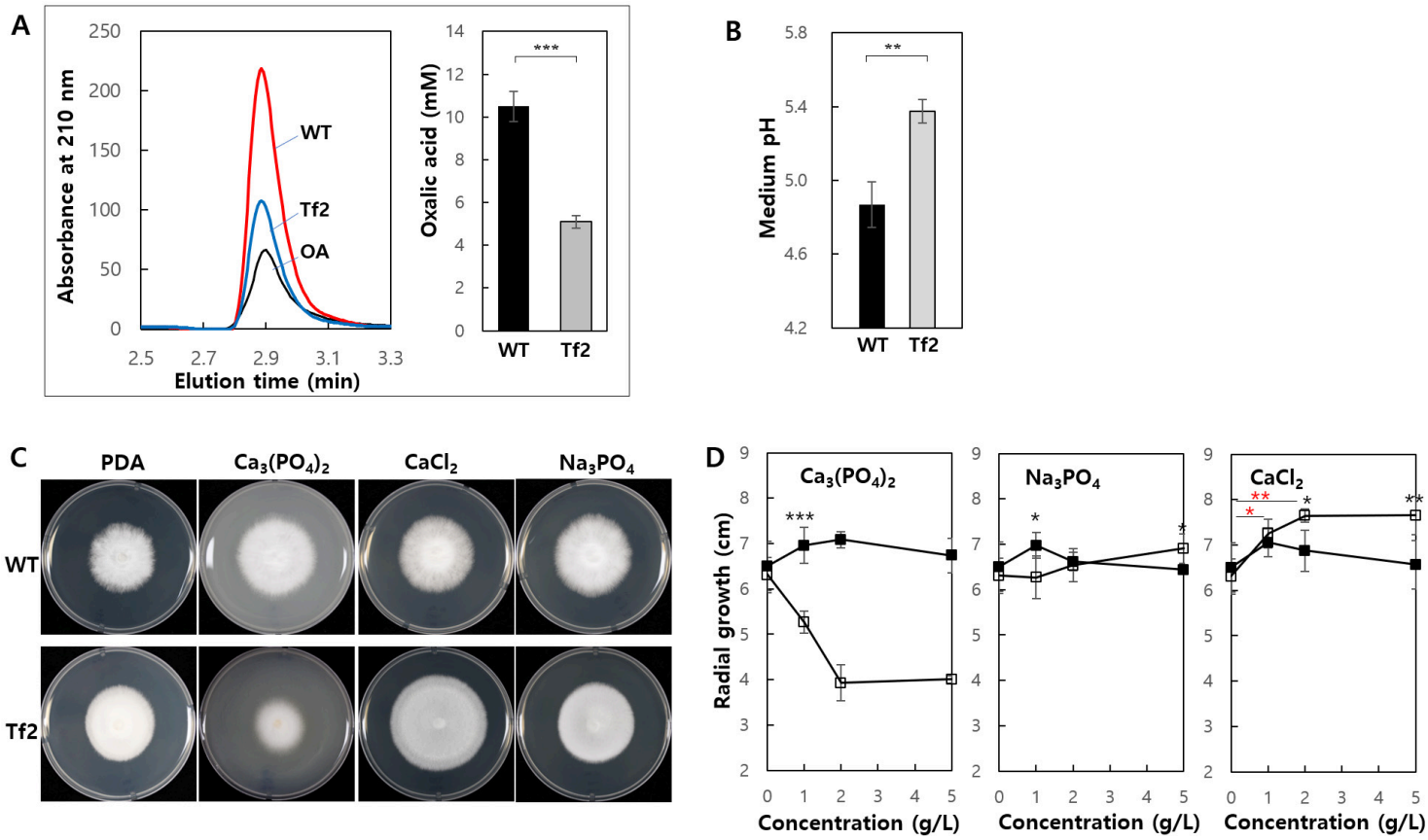


Figure 2

Characterization of the *OAH*-disrupted mutant. (A) Analysis of oxalic acid production by HPLC. Culture broth grown in PDB for 1 week at 30℃ was diluted with the mobile phase (1:4, v/v) and then subjected to HPLC analysis. The concentration of oxalic acid (OA) standard was 0.75 mM. OA concentration of the wild-type M8 strain was 10.5±0.7 mM, whereas that of the *OAH*-disrupted mutant Tf2 was 5.1±0.3 mM. The OA concentrations were calculated using triplicated data sets. (**B)** pH value of culture medium. **(C)** Mycelial growth in the presence of different salts (5 g/L). Radial mycelial growth was measured after 1 week of incubation on PDA at 30℃. **(D)**Concentration-dependent mycelial growth, containing variable concentrations of salts. Error bars represent standard deviations derived from three independent measurements.

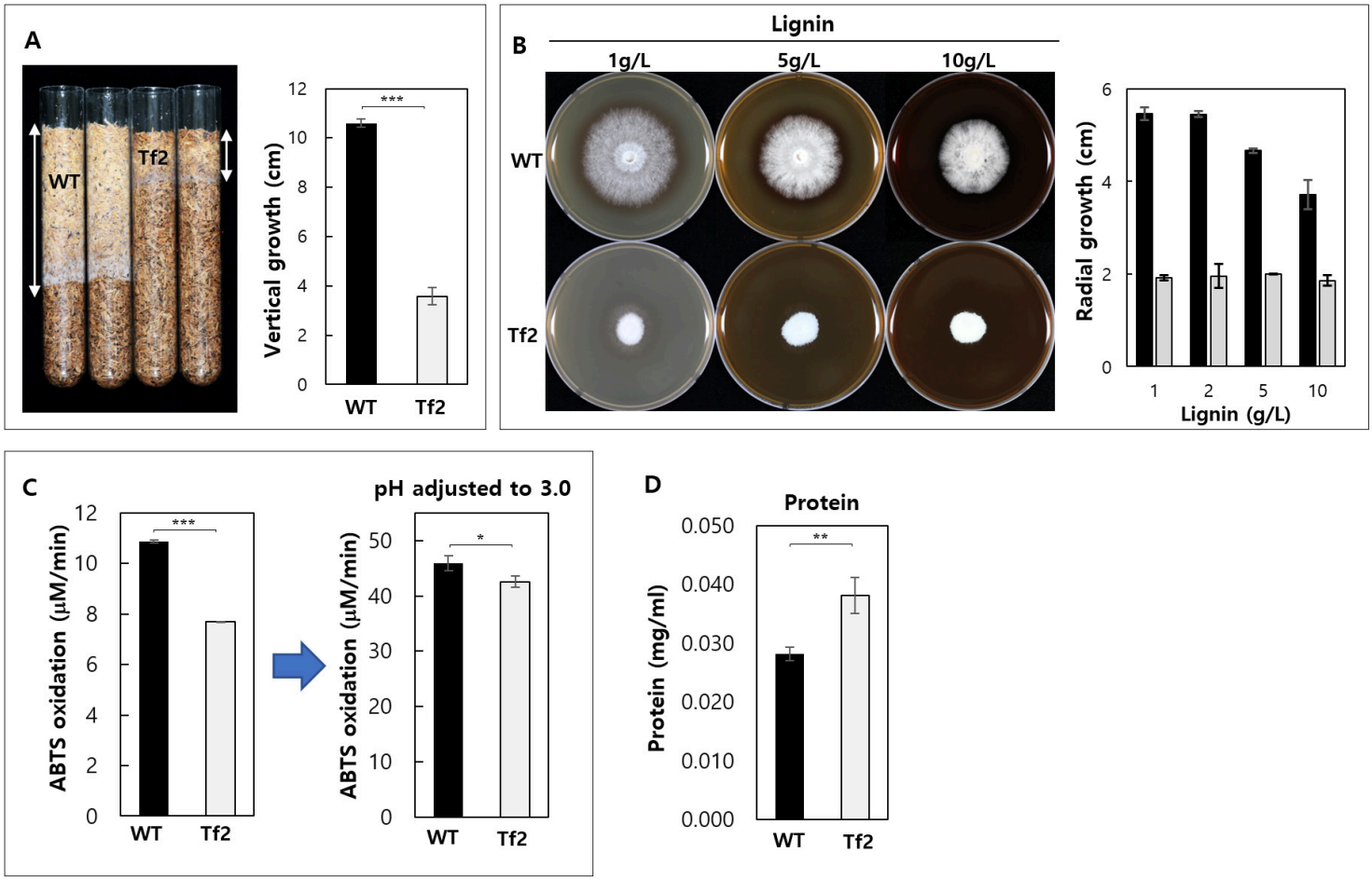


Figure 3

Growth of the *OAH*-disrupted mutant in woody substrate. (A) Mycelial development in sawdust substrate. Mycelial block grown on PDA was inoculated on top of the substrate and was cultured for 2 weeks at 30°C. The distance to the growing edge of mycelial propagation was measured as vertical growth in centimeter. The average vertical growth was calculated using 6 independent experimental sets. **(B)**Utilization of lignin as a sole carbon source. The mycelia of the wild-type and Tf2 were grown in minimal media containing different concentrations of lignin for 1 week at 30°C. The average radial growth was calculated using three independent experimental data. Black bars represent the growth of the wild-type strain, whereas grey bars represent that of the Tf2. **(C)** Combined laccase and peroxidase activity of the culture broth. The filtered culture (0.3ml) was subjected to ABTS oxidation reaction without pH adjustment (left panel). Next, the enzyme activity was measured in a reaction mixture consisted of 50 mM sodium phosphate buffer (pH 3.0), 5 mM ABTS, and diluted culture supernatant (right panel). **(D)** Protein concentration of the culture broth measured by Bradford assay.

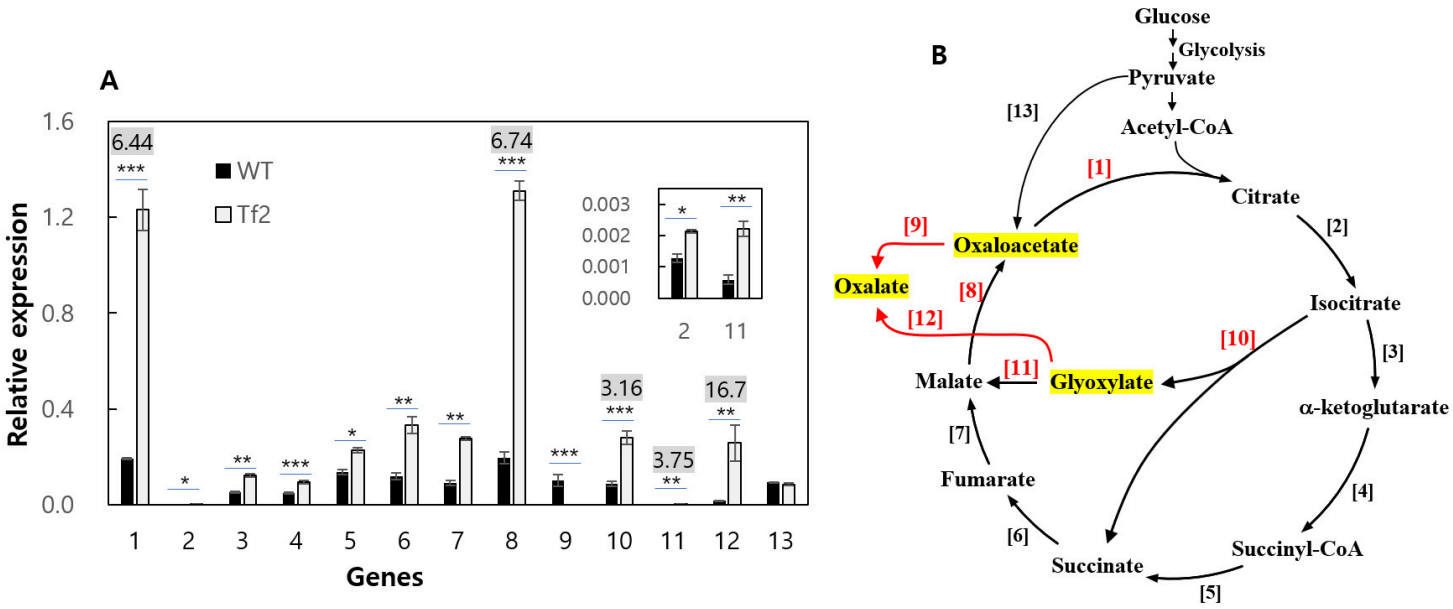


Figure 4

Expression of genes involved in oxalic acid synthesis and related metabolic pathways. (A) Relative expression of selected genes. qRT-PCR was performed using total RNA extracted from mycelia grown in PDB for 1 week at 30°C under static conditions. Black bars represent gene expression in the wild-type (WT) strain, whereas white bars represent expression in the transformant Tf2. Fold changes of selected genes are indicated above the corresponding bars. The inset shows the expression of the low-expressing genes 2 and 11. Relative gene expression was calculated as 2^{-DDCt}. **(B)** Metabolic pathway related to OA production. Genes showing notable changes in expression are highlighted in red. The genes analyzed were citrate synthase (1), aconitase (2), isocitrate dehydrogenase (3), a-ketoglutarate dehydrogenase (4), succinyl CoA synthetase (5), succinate dehydrogenase (6), fumarase (7), malate dehydrogenase (8), oxaloacetate acetylhydrolase (OAH) (9), isocitrate lyase (10), malate synthase (11), glyoxylate oxidase (12), pyruvate carboxylase (13), and tubulin 2 (*tub2*).

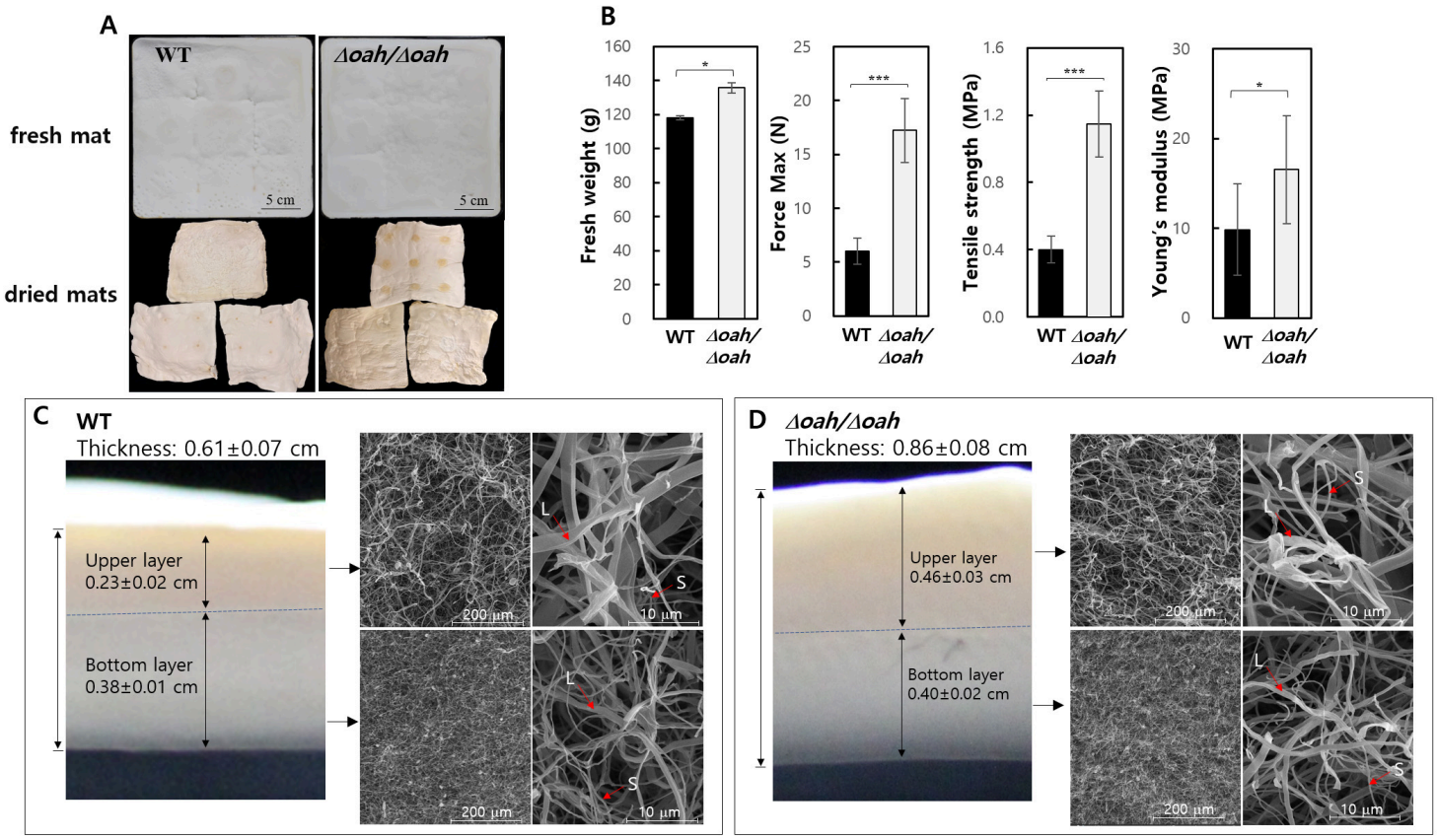


Figure 5

Characterization of mycelial mats. (A) Production of mycelial mats. Fresh mycelial mats (upper panels) were obtained after cultivation on soft PDA in a square dish (24.3 cm × 24.3 cm) for 3 weeks at 30°C. Dried mycelial mats (bottom panels) were generated by fixation with 1% formaldehyde and 5% glycerol, followed by drying at 60°C for 12 h. **(B)** Mechanical properties of the mycelial mats. **(C, D)** Structural characterization of mycelial mats produced by the WT **(C)** and Δ*oah*/Δ*oah* **(D)** strains. Cross-sectional images show the upper and bottom layers of the mycelial mats, and SEM images show the corresponding hyphal structures. Arrows labeled L and S indicate large- and small-diameter hyphae, respectively.

Supplementary Files

This is a list of supplementary files associated with this preprint. Click to download.

- Fig1Bgelimage.png
- SupplementaryDataS1tfseqdata.docx
- SupplementaryTableS1.docx
- graphicalabstract.jpg
- supplementaryFigures.pdf